

# RAMAN SPECTROSCOPY STRUCTURAL STUDY OF FIRED CONCRETE

ŠÁRKA PEŠKOVÁ, #VLADIMÍR MACHOVIČ\*,\*\*, PETR PROCHÁZKA

*Czech Technical University in Prague, Faculty of Civil Engineering,  
Thákurova 7, 166 29 Prague, Czech Republic*

*\*Institute of Chemical Technology Prague, Technická 5, 166 28, Prague, Czech Republic*

*\*\*Institute of Rock Structure and Mechanics v.v.i., ASCR,  
V Holešovičkách 41, 182 09 Prague, Czech Republic*

#E-mail: machoviv@vscht.cz

Submitted February 15, 2011; accepted October 27, 2011

**Keywords:** Fired concrete, Cracks, Raman microspectroscopy

*Raman spectroscopic structural analysis of concrete cementitious matrix represents elegant method to determination of thermal history of highly exposed concrete. Experiments were carried out in furnace at 1200 °C. On the surface of heated concrete mechanical cracks and the mixture of dicalcium silicate and gehlenite were found, while inside the cracks the development of gehlenite, pseudowollastonite, pseudobrookite and various iron oxides and spinels was observed. The products of chemical reactions analyzed by Raman spectroscopy can be used as markers for the identification and understanding the structural changes during a fire treatment.*

## INTRODUCTION

It is well established that mechanical and chemical properties of concrete are adversely affected by thermal exposure. Even in 1920 the factors influencing concrete strength at high temperatures were investigated [1]. Under certain heating conditions, the dehydration of C–S–H gel, the thermal incompatibility between the aggregate and cement paste and the pore pressure within the cement paste had been proved to be the main detrimental factors.

Raman spectroscopy is a spectroscopic technique used to study vibrational, rotational, and other low-frequency modes in a system. It relies on inelastic scattering, or Raman scattering, of monochromatic light, usually from a laser in the visible, near infrared, or near ultraviolet range. It is mentioned in [6-7].

Elevated temperature is very dangerous for different sorts of concrete classes (classification in according to ČSN and STN 206-1) concerning deterioration of material and, consequently, the bearing capacity is principally decreased. Concretes based on Portland pasta reduce the compressive strength during increase of temperature above 200 °C (at 700 °C is the compressive strength only 5% of the initial value). At a high temperature chemical decomposition of calcium-silicate-hydrate occurs, which is the main holder of mechanical properties of the concrete. Portland cement is a heterogeneous mix-

ture of four main compounds: 50-70 % of tricalcium silicate ( $\text{Ca}_3\text{SiO}_5$ ), 20-30 % of dicalcium silicate ( $\text{Ca}_2\text{SiO}_4$ ), 5-12 % tricalcium aluminate ( $\text{Ca}_3\text{Al}_2\text{O}_6$ ), and 5-12 % of calcium aluminoferrite ( $\text{Ca}_4\text{Al}_2\text{Fe}_2\text{O}_{10}$ ). In the cement chemistry these components are abbreviated as:  $\text{C}_3\text{S}$  (alite) for tricalcium silicate;  $\text{C}_2\text{S}$  (belite) for dicalcium silicate;  $\text{C}_3\text{A}$  for tricalcium aluminate and  $\text{C}_4\text{AF}$  for tetracalcium aluminoferrite. The hydration of the dry clinker leads to the prevailing formation: 20-25 % of  $\text{Ca}(\text{OH})_2$  (portlandite, CH), 60-70 % of  $3\text{CaO}\cdot 2\text{SiO}_2\cdot 3\text{H}_2\text{O}$  (calcium-silicate-hydrate, C–S–H gel), and 5-15% of other solid phases, e.g. ettringite [ $\text{Ca}_6\text{Al}_2(\text{SO}_4)_3(\text{OH})_{12}\cdot 26\text{H}_2\text{O}$ ]. C–S–H gel represents the primary binding phase in Portland cement and controls the strength development of the paste [2].

During the course of heating of concrete chemical and physical changes arise as [3]:

- 30-105°C: evaporation of water and part of fixed water. Water is eliminated at 120°C
- 110-170°C: dissociating gypsum ( $\text{CaSO}_4\cdot 2\text{H}_2\text{O}$ ) and ettringite ( $\text{Ca}_6[\text{Al}(\text{OH})_6]_2(\text{SO}_4)_3\cdot 26\text{H}_2\text{O}$ ) yields calcium sulfoaluminum hydrates
- 180-300°C: loss of water from C-S-H gels and hydrates of carboaluminium
- 450-550°C: dehydroxylation of portlandite ( $\text{Ca}(\text{OH})_2$ )
- 700-900°C: decarbonation of calcium carbonate
- above 1150°C feldspar melts and the other minerals of cement paste turn into a glass phase.

Splitting and spalling of parts of composite matrix are related with different thermal expansion of particular components of the concrete mixture, and debond between aggregate and cement paste in consequence of physical and chemical changes occurs. It is particularly the phase change of quartz from triclinic crystal system to the hexagonal system, which happens during the increase of temperature to 570-575°C. Recently, it has been found that the main products of C-S-H decomposition are  $\beta$ -C<sub>2</sub>S and C<sub>3</sub>S. The decay of C-S-H starts at 560°C and decomposition rate increases dramatically with the temperature [4].

The colour of concrete gives general information about the levels of temperature to which the concrete has been exposed. On heating above 300°C the colour of concrete can change from normal to pink (300-600°C) to whitish gray (600-900°C) and buff (900-1000°C). The pink decolouration results from the presence of iron compound [5].

Raman spectroscopy are often useful tools in the characterization of local structure features for solids since these technique allow detection of amorphous as well as crystalline phases by measurement of vibration bands that are sensitive to atomic masses and local symmetry. Raman spectroscopy is an excellent method for identifying compounds, as it provides fingerprint spectra that are unique to each specific substance. Recently an increasing interest has appeared in applying Raman spectroscopy to cementitious systems for exploring the potentials of these materials [6-13].

There is a lack of information concerning the structural changes on the surface of fired concrete in the literature. Raman spectroscopy can be used as a fast and effective analytical tool for the determination of temperature history of concrete after a fire exposure. It can give information about new originated compounds at high temperatures not only on the surface of the fired concrete but also inside the cracks. This paper is focused on the structural changes of concrete cement matrix with fibre reinforced at extremely elevated temperatures.



Figure 1. The surface of fired concrete.

Extreme level of the temperature is 1200°C, according to the European standards.

## EXPERIMENTAL

A specific concrete mixture was prepared using ordinary Portland cement. The concrete mixture of composition is specified in Table 1. The concrete contained 1% of basalt fibres from Russia with diameter of 1  $\mu$ m and length of 50 mm. Mechanical properties of mentioned concrete are described in Table 2.

The high temperature experiments were carried out in a blast furnace with approximate dimensions 1400  $\times$  2200  $\times$  1300 mm and the concrete blocks had dimensions 800  $\times$  600  $\times$  500 mm. Two samples were tested in this experimental part, namely a standard concrete and FRC with basalt fibres. The block is equipped by analog instruments, thermopiles, the gas heater OLYMP 3520, etc. The results obtained here are attained under the time dependent boundary conditions applied on the heated surface of the sample from a concrete blocks. The boundary conditions are selected in such a way that in the first 30 minutes the temperature of 1200°C is successively attained and another 90-120 minutes this boundary temperature is kept. Then the source of heating is removed and a natural cooling process is initiated until the room temperature is attained. The photo of the concrete block is shown in Figure 2.

Table 1. Masses of constituents in dry aggregate concrete C40/50 with basalt fibers.

Constituent .....	1 m <sup>3</sup> concrete mixture
Cement I 52,5 R, Radotín .....	560 kg
Sand 0-4 mm from Hostín .....	800 kg
Aggregate 4-8 mm from Hostín .....	820 kg
Water .....	180 l
Superplasticizer 0800- Pantarhit, producer- Ha-Be Betonchemie s.r.o .....	6 l
Basalt fibers - diameter 1 $\mu$ m, length 50 mm, supplier-Kamenny Vek (Russia) .....	20 kg

Table 2. Properties of concrete C40/50 with basalt fibers.

$f_{ck}$ [MPa] (compressive strength) .....	40
$f_{cm}$ [MPa] (compressive strength) .....	48
$f_{ctm}$ [MPa] (tensile strength) .....	3.5
$f_{ctk 0,05}$ [MPa] (tensile strength) .....	2.5
$f_{ctk 0,95}$ [MPa] (tensile strength) .....	4.6
$E_{cm}$ [GPa] .....	35
$\epsilon_{cu} \times 10^{-4} \text{‰}$ (ultimate concrete deformation - for bearing capacity) .....	-3.0
$\epsilon_{cu} \times 10^{-4} \text{‰}$ (ultimate concrete deformation - impact loads in concrete) .....	-3.5

Raman microspectra have been measured by Raman dispersive spectrometer (fy Jobin Yvon model Labram HR) which is equipped with confocal microscope Olympus. As an excitation source a laser (Model Compass 315M) with the wave length 532.2 nm and input power 50 mW was used. Specimens were measured with parameters: power 0.5 mW, measuring time 30 s and 64 accumulations of spectrum. These parameters were adjusted in such a way that the thermal destruction of samples became impossible. Other information concerning the test is recorded as: grating - 600 gr/mm, aperture of split 150, hole 1000, spatial resolution:  $\sim 2$  micrometer, and a multichannel, air-cooled CCD camera served as a detector. Hereafter discussed Raman spectra involve representative measurements of five points.

## RESULTS AND DISCUSSION

### Raman spectra of the original concrete

The Raman spectra of original hydrated concrete cement matrix after one year 20°C water cure are shown in Figures 2 and 3. The spectra were recorded by selectively focusing on the surface of the selected particles having different colours. The objective enabling 50 $\times$  zoom corresponds to a sample area of *ca.* 2  $\mu$ m diameter.

Figure 2 displays the Raman spectra of the white particles of the one year hydrated concrete cement paste, which are located inside of the cracks. The bands at 881, 908 and 953  $\text{cm}^{-1}$  (see Figure 2, spectrum A and B) can be assigned to  $\nu_1(\text{SiO}_4)$  symmetric stretching vibration of C-S-H gel, which is the main phase formed during cement hydration. The complex broad band in the 620-690  $\text{cm}^{-1}$  region may be attributed to formation of poorly crystalline calcium silicate hydrates (C-S-H gels) [10-14]. The band centered at  $\sim 670$   $\text{cm}^{-1}$  has previously been identified in synthetic C-S-H as arising from Si-O-Si bending modes involving  $\text{Q}_2$  tetrahedra. The other C-S-H low intensity bands can be found at  $\sim 316$   $\text{cm}^{-1}$  (lattice vibrations of Ca-O) and at  $\sim 443$   $\text{cm}^{-1}$  (symmetric bending  $\nu_2$  (Si-O). Small band at 365  $\text{cm}^{-1}$  is ascribed to residual portlandite -  $\text{Ca}(\text{OH})_2$ .

Carbonation of C-S-H phase involves structural changes yielding  $\text{Q}_2$  silicate species in consequence of polymerization of the silicate dimers. The  $\text{Q}_2$  silicate chains are only short, as indicated by the continued appearance of a prominent band at 880  $\text{cm}^{-1}$ . The shoulder of the band at 998  $\text{cm}^{-1}$  can be assigned to symmetric  $\text{SO}_4$  stretching modes of the ettringite and the band at 1012  $\text{cm}^{-1}$  to gypsum [10]. In the spectra of some white particles accompanying four bands at 144, 392, 512 and 636  $\text{cm}^{-1}$  of anatase (see Figure 6, spectrum B) were found. Note that Raman spectroscopy has been increasingly used in the studies of carbonation reaction in

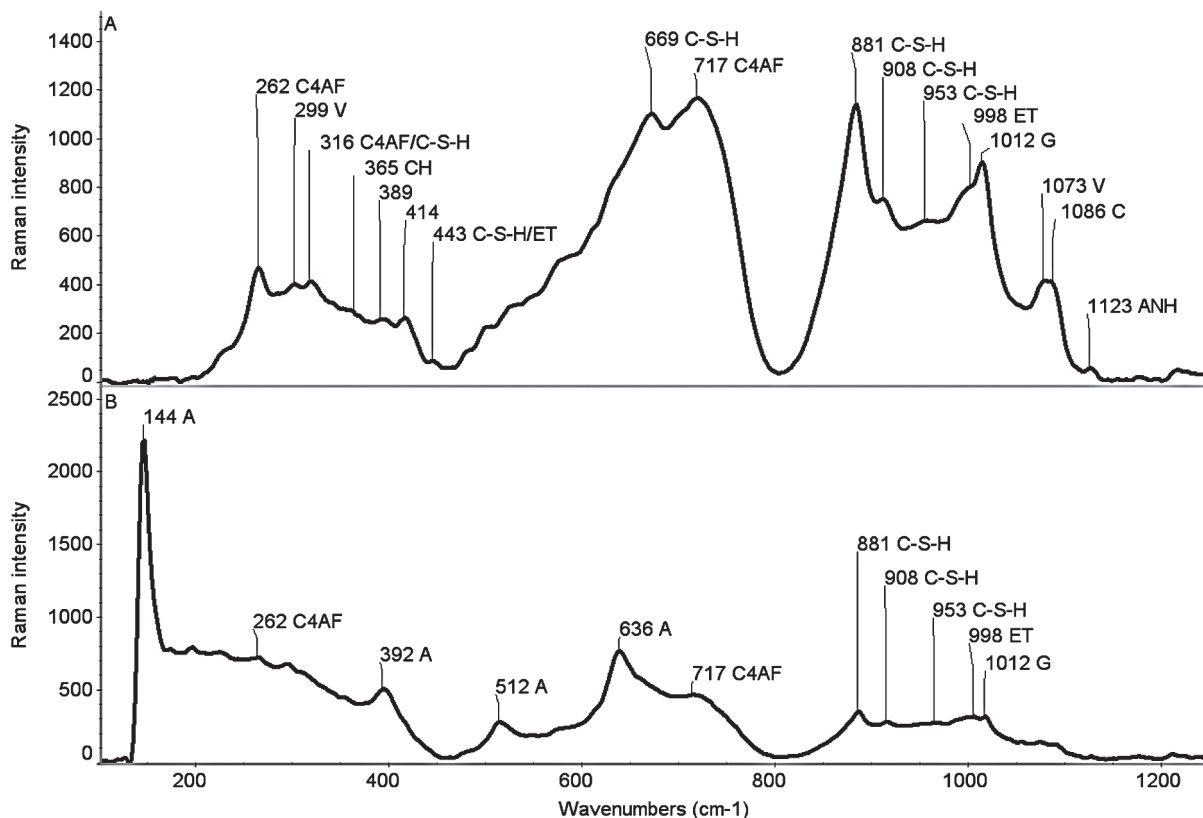


Figure 2. Raman spectra of white particles of original concrete.

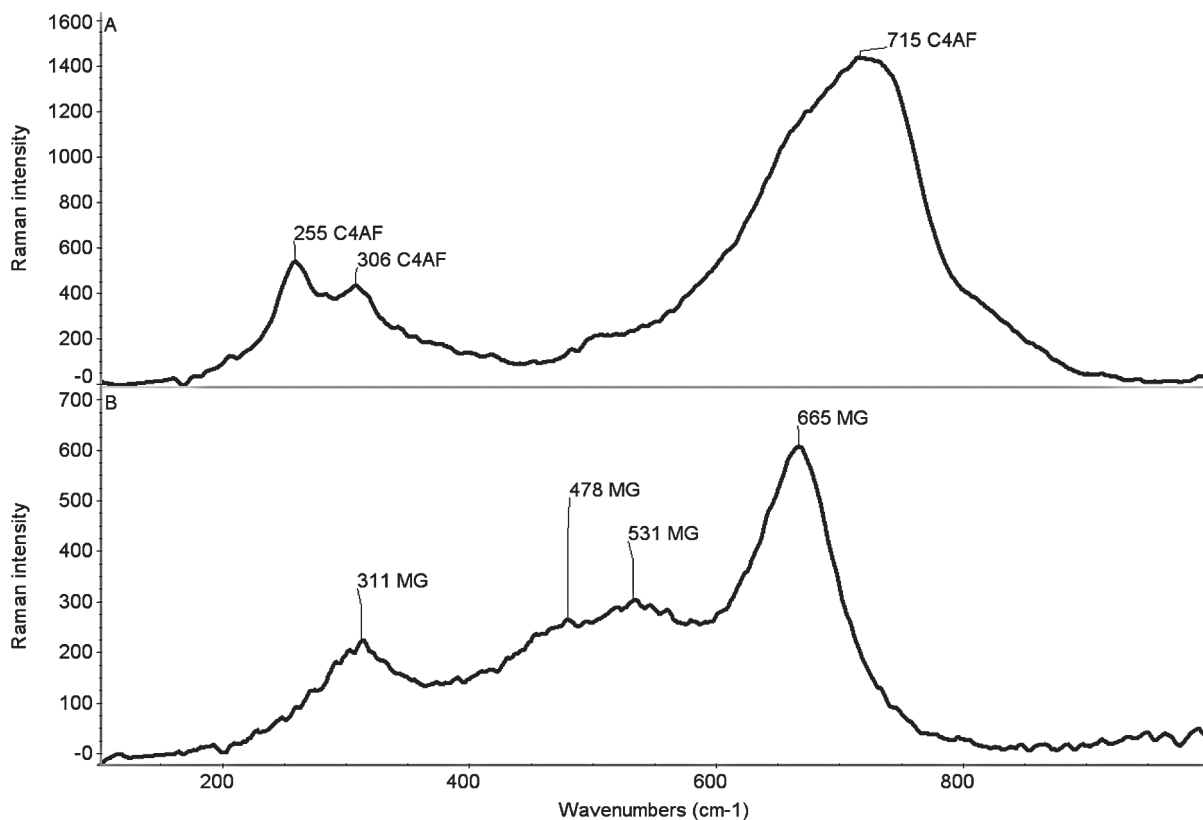


Figure 3. Raman spectra of dark particles of original concrete.

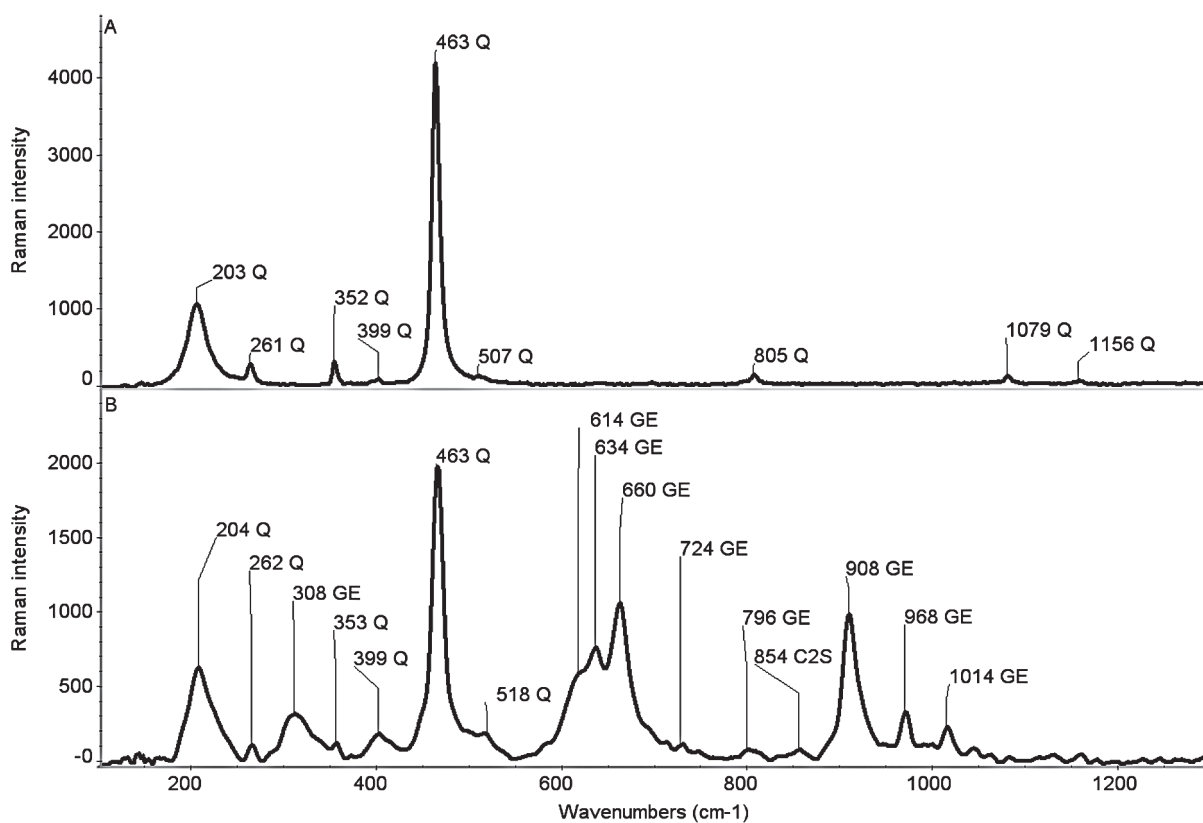


Figure 4. Raman spectra of the fired concrete (A - dark particle in the crack, B - white particle in the crack).

cementitious materials. The three polymorph of  $\text{CaCO}_3$  (i.e. calcite, aragonite and vaterite) can be distinguished from their Raman spectra. The increase amount of calcium carbonate in concrete may be identified by the increase in intensity of the  $\nu_1[\text{CO}_3^{2-}]$  band at  $1080\text{ cm}^{-1}$  and by the observation the  $\nu_4[\text{CO}_3^{2-}]$  band. The curve fitting the complex band in the Raman spectrum of analyzed concrete matrix centered at  $\sim 1080\text{ cm}^{-1}$  revealed two band of vaterite at  $1075\text{ cm}^{-1}$  and calcite at  $1086\text{ cm}^{-1}$  [12]. The band positions of the phases identified in origin and fired concrete are summarized in Table 3.

The Raman spectrum of the dark particles (see Figure 3, spectrum A) shows a broad intensive band centered at  $715\text{ cm}^{-1}$  and two low intensity bands at  $255$  and  $306\text{ cm}^{-1}$ . The spectrum is typical for aluminoferrite ( $\text{C}_4\text{AF}$ ) particles in the original concrete cement paste [10, 12]. The broad band around  $700\text{ cm}^{-1}$  is assigned to the  $\nu_1$  vibration of  $[(\text{Fe,Al})\text{O}_4]^{5-}$  groups. Minor bands centered at  $255$  and  $306\text{ cm}^{-1}$  are assigned to  $\nu_2$  and  $\nu_4$  of the  $[(\text{Fe,Al})\text{O}_4]^{5-}$ . The broad band in the  $700\text{--}730\text{ cm}^{-1}$  region reflects the fact that  $\text{C}_4\text{AF}$  can encompass a range

of solid solutions of various Ca-Al-Fe-O content [10]. The spectrum b in Figure 3, taken for dark particle, is typical for magnetite  $\text{Fe}_3\text{O}_4$ .

#### Raman spectra of the fired concrete

The cement paste undergoes a continuous sequence of more or less irreversible decomposition reaction during the heating. As can be seen in Figures 4-7, the spectra of the concrete paste specimen subjected to a temperature of  $1200^\circ\text{C}$ , are quite different from the spectra of original concrete matrix and consequently may be assumed that deterioration of the concrete takes place. The C-S-H gel, which is the strength giving compound of the concrete decomposes above  $600^\circ\text{C}$ , at  $800^\circ\text{C}$ , concrete is usually crumbled and cracked and above  $1150^\circ\text{C}$  turn into a glass phase [15]. This gel is determined inside the crack of concrete, where the temperature was below  $200^\circ\text{C}$ . The structure of the reaction products can be used as a marker for the assignment of the thermal history of the concrete during burning [4].

Table 3. Band positions of the principal phases identified in origin and fired concrete. The most intensive vibrational modes are marked in bold.

Phase	Band position ( $\text{cm}^{-1}$ )	Figure	Abbreviations
<b>origin concrete</b>			
anatase $\text{TiO}_2$	144, 392, 512, 636	2B	A
anhydrite $\text{CaSO}_4$	1123	2A	ANH
$\text{Ca}(\text{OH})_2$	365	2A	CH
calcite $\text{CaCO}_3$	1086	2A	C
calcium aluminoferrite $\text{C}_4\text{AF}$	262, 316, 717	2A, 2B, 3A	$\text{C}_4\text{AF}$
C-S-H	316, 443, 669, 881, 908, 953	2A, 2B	C-S-H
ettringite $\text{Ca}_6\text{Al}_2(\text{SO}_4)_3(\text{OH})_{12}\cdot 26\text{H}_2\text{O}$	998, 443	2A, 2B	ET
gypsum $\text{CaSO}_4\cdot 2\text{H}_2\text{O}$	1012	2A, 2B	G
magnetite $\text{Fe}_3\text{O}_4$	311, 478, 531, 665	3B	MG
vaterite $\text{CaCO}_3$	299, 1073	2A	V
<b>fired concrete - inside of the cracks</b>			
A-dark particle in crack			
B-white particle in crack			
belite $\text{C}_2\text{S}$	164, 226, 301, 513, 854, 890, 980	4B, 5A, 5B	$\text{C}_2\text{S}$
gehlenite $\text{Ca}_2\text{Al}_2\text{SiO}_7$	308, 614, 634, 660, 724, 796, 908, 968, 1014	4B, 5A, 5B	GE
hematite $\text{Fe}_2\text{O}_3$	211, 272, 375, 480, 581	6B	H
maghemite $\alpha\text{-Fe}_2\text{O}_3$	713	6A	MH
nonstoichiometric pseudobrookite $\text{Fe}_2\text{TiO}_5$	343	5B	PB
pseudowollastonite $\alpha\text{-CaSiO}_3$	182, 307, 318, 333, 367, 505, 553, 575, 992, 982, 1068	5A	PW
quartz $\text{SiO}_2$	203, 261, 352, 399, 463, 507, 1079, 1156	4A, 4B, 5A, 5B	Q
Spinel $(\text{M}^{2+}, \text{Fe}^{2+})(\text{M}^{3+}, \text{Fe}^{3+})_2\text{O}_4$	610	5B, 6A	F
<b>fired concrete - surface</b>			
belite $\text{C}_2\text{S}$	201, 221, 252, 369, 421, 533, 557, 856, 889, 975	7A	$\text{C}_2\text{S}$
gehlenite $\text{Ca}_2\text{Al}_2\text{SiO}_7$	308, 369, 624, 658	7A	GE
anhydrite $\text{CaSO}_4$	1123	7A	ANH
vaterite $\text{CaCO}_3$	1074	7A	V

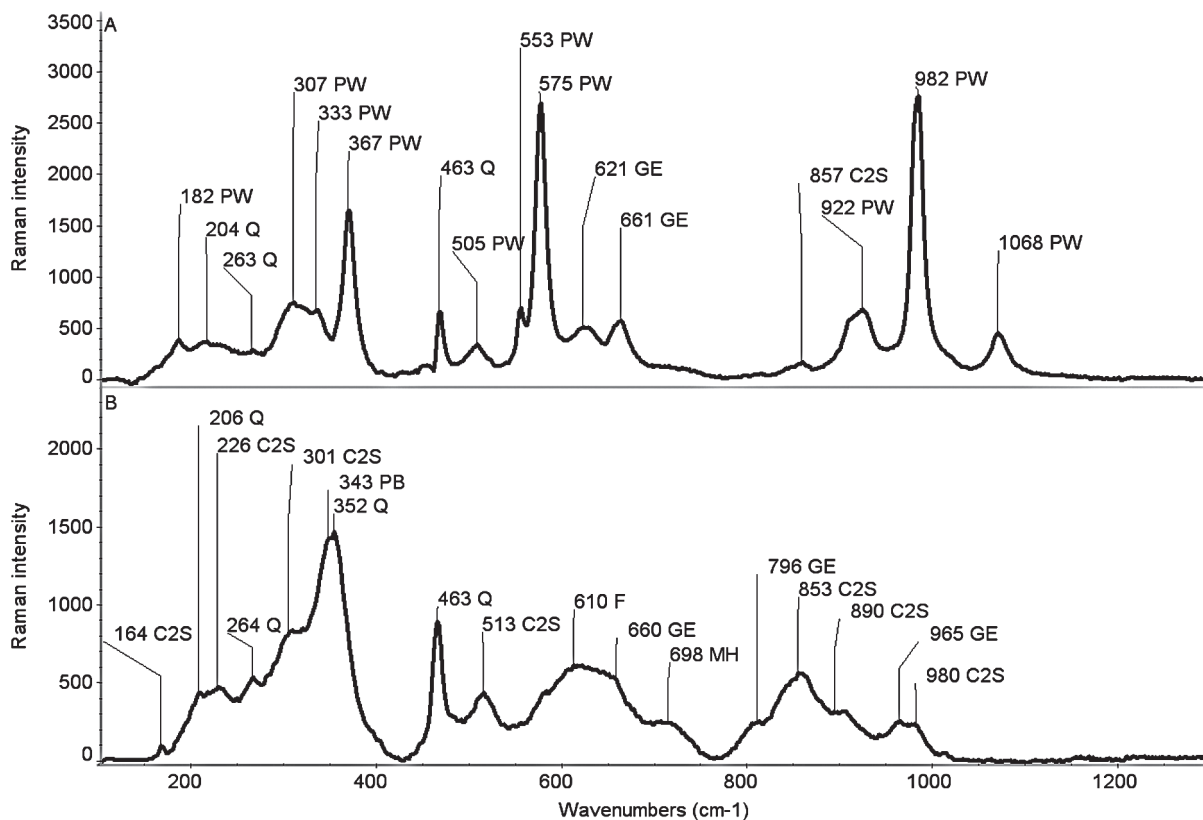


Figure 5. Raman spectra of the fired concrete (A, B - white particles in the crack).

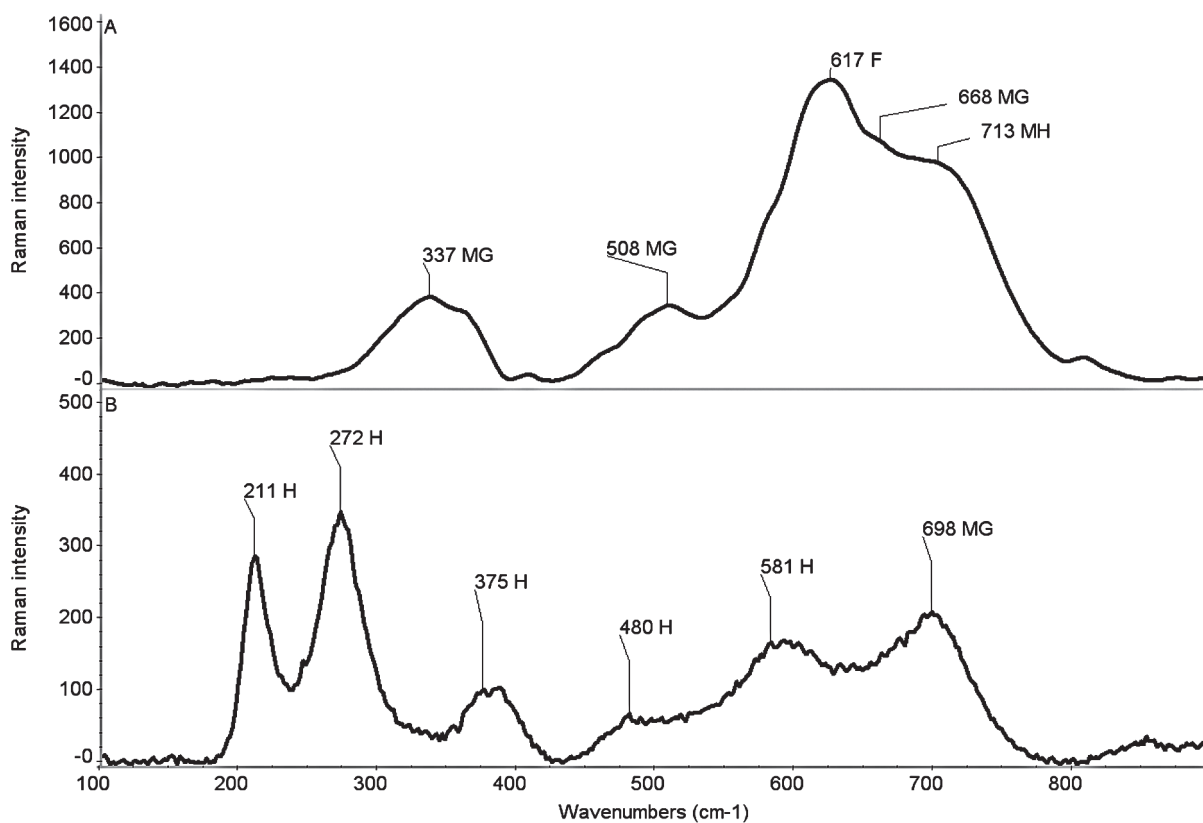


Figure 6. Raman spectra of the fired concrete (A, B - dark particles in the crack).

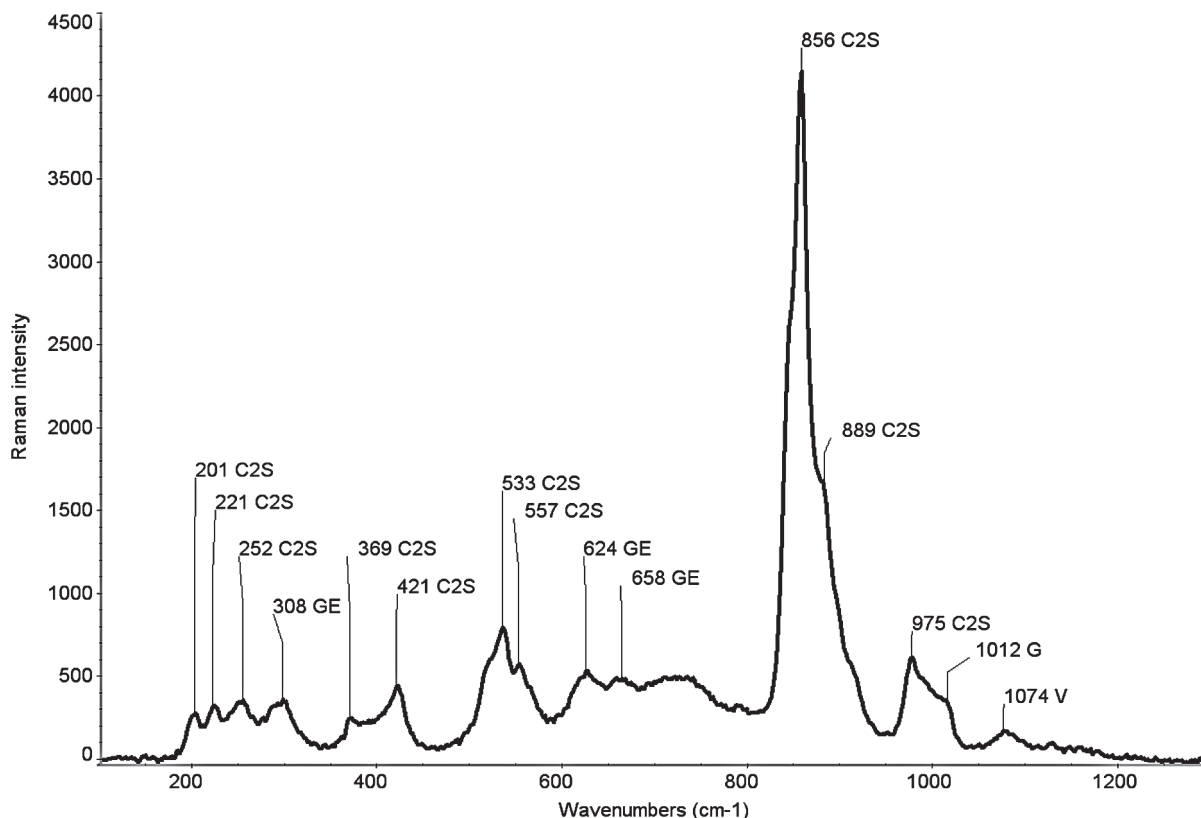


Figure 7. Raman spectrum of the white particle on the surface of the fired concrete.

Figure 4A shows the Raman spectrum of brown dark particle inside the crack. From the prominent band at  $463\text{ cm}^{-1}$  and further bands at  $203$ ,  $261$ ,  $352$ ,  $399$ ,  $507$ ,  $805$ ,  $1079$  and  $1156\text{ cm}^{-1}$  the spectrum can be assigned to quartz with no polymorphic transformation. On the surface of concrete, the air humidity passes from  $\text{CaO}$  to  $\text{Ca}(\text{OH})_2$ . In the Raman spectrum (see Figure 4B) of white particle taken from the same crack can be seen the prominent band at  $908\text{ cm}^{-1}$  can be seen and the small band at  $968\text{ cm}^{-1}$  assigned to symmetric stretching mode of the non-bridging oxygen of the phyllosilicate groups of the gehlenite ( $\text{Ca}_2\text{Al}_2\text{SiO}_7$ ) [16]. The bands at  $614$  and  $634\text{ cm}^{-1}$  are ascribed to mixed bending and stretching mode of T–O–T (where T=Si or Al) bonds in gehlenite and the intensive band at  $660\text{ cm}^{-1}$  and small bands at  $724$  and  $796\text{ cm}^{-1}$  are assigned to symmetric stretching of  $\text{AlO}_4$ . The band at  $1014\text{ cm}^{-1}$  is determined by asymmetric stretching of Si–O–Al and the band at  $308\text{ cm}^{-1}$  may be attributed to lattice gehlenite mode. Other bands in spectrum are due to quartz ( $204$ ,  $262$ ,  $353$ ,  $399$ ,  $463$ ,  $518\text{ cm}^{-1}$ ). The small band at  $854\text{ cm}^{-1}$  is assigned to belite  $\text{C}_2\text{S}$ .

Among further compounds found in cracks pseudowollastonite ( $\alpha\text{-CaSiO}_3$ ) was discovered, which is the high temperature polymorph of the natural chain-silicate mineral wollastonite. At high frequencies, the three bands observed (see Figure 5A) at  $922$ ,  $982$  and

$1068\text{ cm}^{-1}$  represent mainly Si–O stretching modes, [17]. Mid frequencies bands at  $553$  and  $575\text{ cm}^{-1}$  are assigned to Si–O–Si bending and Si–O stretching modes, and low wavenumbers bands at  $182$ ,  $307$ ,  $333$  and  $505\text{ cm}^{-1}$  represent deformation of the silicate network along with Ca–O stretching. In addition to the band of pseudowollastonite, the bands of the quartz, gehlenite and  $\text{C}_2\text{S}$  can be found in the spectrum.

The spectrum B in Figure 5 shows the prominent broad band at  $343\text{ cm}^{-1}$ , which was tentatively assigned to nonstoichiometric pseudobrookite -  $\text{Fe}_2\text{TiO}_5$ . The bands of the belite, quartz, gehlenite and maghemite can be seen in the spectrum.

The Raman spectrum in Figure 6A can be assigned to the mixture of magnetite ( $337$ ,  $508$  and  $668\text{ cm}^{-1}$ ) and maghemite (band at  $713\text{ cm}^{-1}$ ). The band at  $617\text{ cm}^{-1}$  was tentatively identified as spinel ( $\text{M}^{2+}$ ,  $\text{Fe}^{2+}$ )( $\text{M}^{3+}$ ,  $\text{Fe}^{3+}$ ) $_2\text{O}_4$ . The spectra of dark particles in the crack (see Figure 6B) show modes at  $211$ ,  $272$ ,  $375$ ,  $480$ ,  $581$  and  $698$  which can be ascribed to a mixture of low crystalline hematite/magnetite [18].

In the Raman spectrum of the prevailing white surface of concrete cement matrix particles the band at  $855\text{ cm}^{-1}$  with shoulders at  $880$  and  $840\text{ cm}^{-1}$  dominated, Figure 7. This can be assigned to a symmetric stretching mode of belite - dicalcium silicate ( $\text{Ca}_2\text{SiO}_4$ ), [15]. Further the band of belite can be found at  $974\text{ cm}^{-1}$

(asymmetric stretching of the SiO<sub>4</sub>), triplet at 557, 533 and 515 cm<sup>-1</sup> (asymmetric SiO<sub>4</sub> bending) and at 421 and 369 cm<sup>-1</sup> (SiO<sub>4</sub> bending). In the spectrum of belite bands of gehlenite at 623, 658 and 905 cm<sup>-1</sup>, sulphate and carbonate at 1014 and 1074 cm<sup>-1</sup>, respectively, can also be found.

Raman microspectroscopy has been thus applied successfully to the characterization of the main substances presented on the concrete cement matrix surface and in the cracks of the fired concrete, giving clear and not entire overlapping spectral features. Next work will be aimed at the Raman microspectroscopic analysis of the various substances picked up from laboratory concrete samples exposed to temperature ranging from 100 to 1200°C or on real specimens taken from the fired buildings or tunnels.

### CONCLUSIONS

Raman microspectroscopy is useful and efficient application in the field of the fired concrete. All analyzed phases show very intense Raman scattering, and each of them is characterized by a well-defined and unique Raman spectrum that acts like a fingerprint for its identification of the fired concrete samples of unknown burning history. The Raman microprobe instrument allows analysis of the coloured particles on the micrometer level not only on the surface of the fired concrete cement matrix but inside of the cracks, arises from the temperature volume changes of the cement paste and aggregates. The spectra of concrete specimen subjected to a temperature of 1200°C were thoroughly different from the spectra of original concrete due to its complete deterioration. Inside of the mechanical cracks being observed in the neighborhood of the heated surface the gehlenite, pseudowollastonite, dicalcium silicate pseudobrookite and various iron oxides and spinels were found. On the surface of fired concrete mainly the mixture of the dicalcium silicate and gehlenite was found. The reaction products analyzed by Raman spectroscopy can be used as markers for the determination and understanding of thermal history of concrete in fired buildings or tunnels.

### Acknowledgement

*Thanks are due to Technical University of Innsbruck, personally to Professors Swoboda and Paulini, for fruitful cooperation and enabling Dr. Pešková to conduct certain experiments using their blast furnace.*

*This work has been prepared under support of grant projects of the Grant Agency of the Czech Republic No. 103/09/P541, P104/10/2344, and within the framework of the research center CIDEAS, No. 1M0579.*

### References

1. Lea F.C., Stradling R.: *Engineering 114*, 341, 380 (1922).
2. Ramachandran V. S., Beaudoin J. J.: *Handbook of analytical techniques in concrete science and technology*, Principles, Techniques, and Applications, William Andrew Publishing/Noyes Publications, Norwich, New York 2001.
3. Alarcon-Ruiz L., Platret G., Massien E., Ehrlacher A.: *Cement Concr. Res.* 35, 609 (2005).
4. Peng G.P., Huang Z.S.: *Construction and building materials* 22, 593 (2008).
5. Georgali B., Tsakiridis P.E.: *Cement and Concrete Composites* 27, 255 (2005).
6. Machovič V., Kolář F., Procházka P., Pešková Š., Kuklík P.: *Acta geodynamica et geomaterialia*. 3, 63 (2006).
7. Machovič V., Kopecký L., Němeček J., Kolář F., Svitilová J., Bittnar Z., Andertová J.: *Ceramics-Silikaty* 52, 54 (2008).
8. Machovič V., Andertová J., Kopecký L., Černý M., Borecká L., Příbyl O., Kolář F., Svitilová J.: *Ceramics-Silikaty* 52, 172 (2008).
9. Potgieter-Vermaak S. S., Potgieter J. H., Belleil M., DeWeerd F., Van Grieken R.: *Cem. Concr. Res.* 36, 656 (2006).
10. Deng C.-S., Breen C., Yarwood J., Habesch S., Phipps J., Craster R., Maitland G.: *J. Mat. Chem.* 11, 3105 (2002).
11. Tarrida M., Madon M., Le Rolland B., Colombet P.: *Advn. Cem. Bas. Mat.* 2, 15 (1995).
12. Martinez-Ramirez S., Frías M., Domingo C.: *J. Raman Spectrosc.* 37, 555 (2006).
13. Black L., Breen Ch., Yarwood J., Gargev K., Stemmermann P., Gasharova B.: *J. Am. Ceram. Soc.* 90, 908 (2007).
14. Kirkpatrick R.J., Yarger J.L., McMillan P. F., Yu P., Cong X.: *Advn. Cem. Bas. Mat.* 5, 93 (1997).
15. Arioiz O.: *Fire Safety Journal* 42, 8, 516 (2007).
16. Sharma S. K., Simons B., Yoder Jr. H.S.: *American Mineralogist* 68, 1113 (1983).
17. Richet P., Mysen B. O., Ingrin J.: *Phys. Chem. Minerals* 25, 401 (1998).
18. Chourpa I., Douziech-Eyrolles L., Ngaboni-Okassa L., Fouquenot J. F., Cohen-Jonathan, Martin Soucé S., Marchais H., Dubois P.: *Analyst* 130, 1395 (2005).